

ELECTROMAGNETIC AND BEAM DYNAMICS MODELING OF THE LANSCE COUPLED-CAVITY LINAC WITH CST STUDIO

S. S. Kurennoy[†], Y. K. Batygin, Los Alamos National Laboratory, Los Alamos, NM, USA

Abstract

The 800-MeV proton linac at the Los Alamos Neutron Science Center (LANSCE) includes a drift-tube linac, which brings the beam to 100 MeV, followed by a coupled-cavity linac (CCL) consisting of 44 modules. Each CCL module contains multiple tanks, and it is fed by a single 805-MHz klystron. CCL tanks are multi-cell blocks of identical re-entrant side-coupled cavities, which are followed by drifts with magnetic quadrupole doublets. Bridge couplers – special cavities displaced from the beam axis – electromagnetically couple CCL tanks over such drifts. We have developed 3D CST models of CCL tanks. The RF fields in the tanks are calculated with MicroWave Studio, and magnetic fields of quadrupole doublets are found with ElectroMagnetic Studio. Beam dynamics is modeled with Particle Studio for bunch trains with realistic beam distributions using the CST calculated fields to determine the output beam parameters. Beam dynamics results are compared with other multi-particle codes and provide data for training physics-based surrogate models.

INTRODUCTION

Realistic 3D models of accelerator structures proved to be useful for studying various EM effects, mechanical tolerances, and beam dynamics. Some examples are referenced in [1]. We applied modeling with CST Studio [2] to the LANSCE coupled cavity linac (CCL). As a first step, we built a simplified CST model of the first CCL tank (T1) in the module 5 (M5T1). The model is fully parametrized and applicable for all tanks in the CCL modules [1]. All geometrical and design electromagnetic parameters of the LANSCE CCL cavities are summarized in the original 1968 document [3]. Here we extend our CST modeling by adding more realistic CCL tank fields and magnetic quadrupole fields. The CST results are used for comparison with other beam dynamics codes, e.g., BeamPath [4].

CST MODELING OF CCL

EM Model of Module 5 Tank 1 (M5T1)

The first module of CCL, module 5 (M5; the count includes four preceding DTL modules), starts at beam energy of 100 MeV and consists of four tanks. Each tank in M5 contains 36 identical (within the tank) re-entrant accelerating cavities (cells, AC), which are side coupled by 35 coupling cavities (CC). The coupling cavities are located off axis (side-coupled structure) and alternate their transverse positions on both sides of the beam path, see in Figs. 1-2. Drifts after each tank contain a doublet of two EM quadrupole magnets. For M5T1, the AC length is $\beta\lambda/2 = 8.0274$

cm, where $\beta = v/c = 0.4311$ and $\lambda = 37.242$ cm for 805 MHz, and AC inner radius 12.827 cm. The tank total length is 289 cm, and the drift after T1 is 72.3 cm.

Vacuum volume and fields in one structure period are shown in Fig. 1 and for the whole tank M5T1 in Fig. 2. The cavity frequency is tuned to the frequency 805 MHz of the operating π -mode by adjusting the AC gap. In practice, some additional metal was left on the drift-tube noses of manufactured half-cavities, and it was scraped by a special tool to adjust the frequency before cavity brazing.

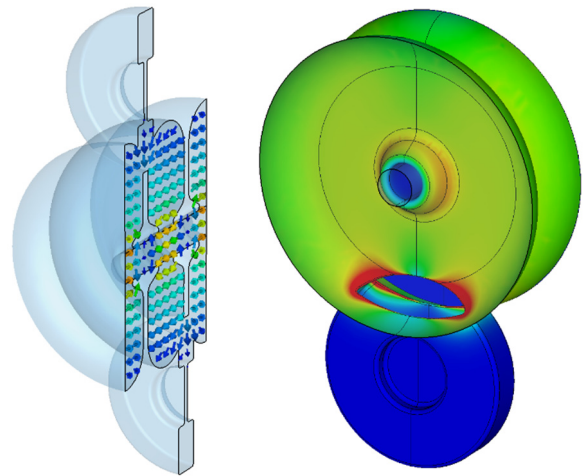


Figure 1: Electric field in one period (left) and surface-current magnitude on the cavity inner surface (right). Red color indicates higher values, blue – lower ones.

The end cell at the tank entrance, Fig. 2 (top, left), has a shorter gap in its left half-cell to keep the π -mode field at the same amplitude along the tank, Fig. 2 (bottom). Some calculated EM parameters of M5T1 are summarized in Table 1. The fields and power (100% duty) are scaled to the nominal accelerating gradient of $E_0T = 1.37$ MV/m and assume ideal copper surface with $\sigma = 5.8 \cdot 10^7$ Sm/m.

Table 1: Calculated EM Parameters of M5T1

Parameter	Value	Units
Quality factor Q	17630	
Transit-time factor T ($\beta = 0.4311$)	0.862	
Energy gain per AC	0.110	MeV
Effective impedance $Z_{\text{eff}} = R_{\text{sh}}T^2/L$	31.45	M Ω /m
Averaged power dissipation per AC	4.79	kW
Maximum peak electric field	8.3	MV/m
Max peak surface magnetic field	27.4	kA/m

[†] kurennoy@lanl.gov

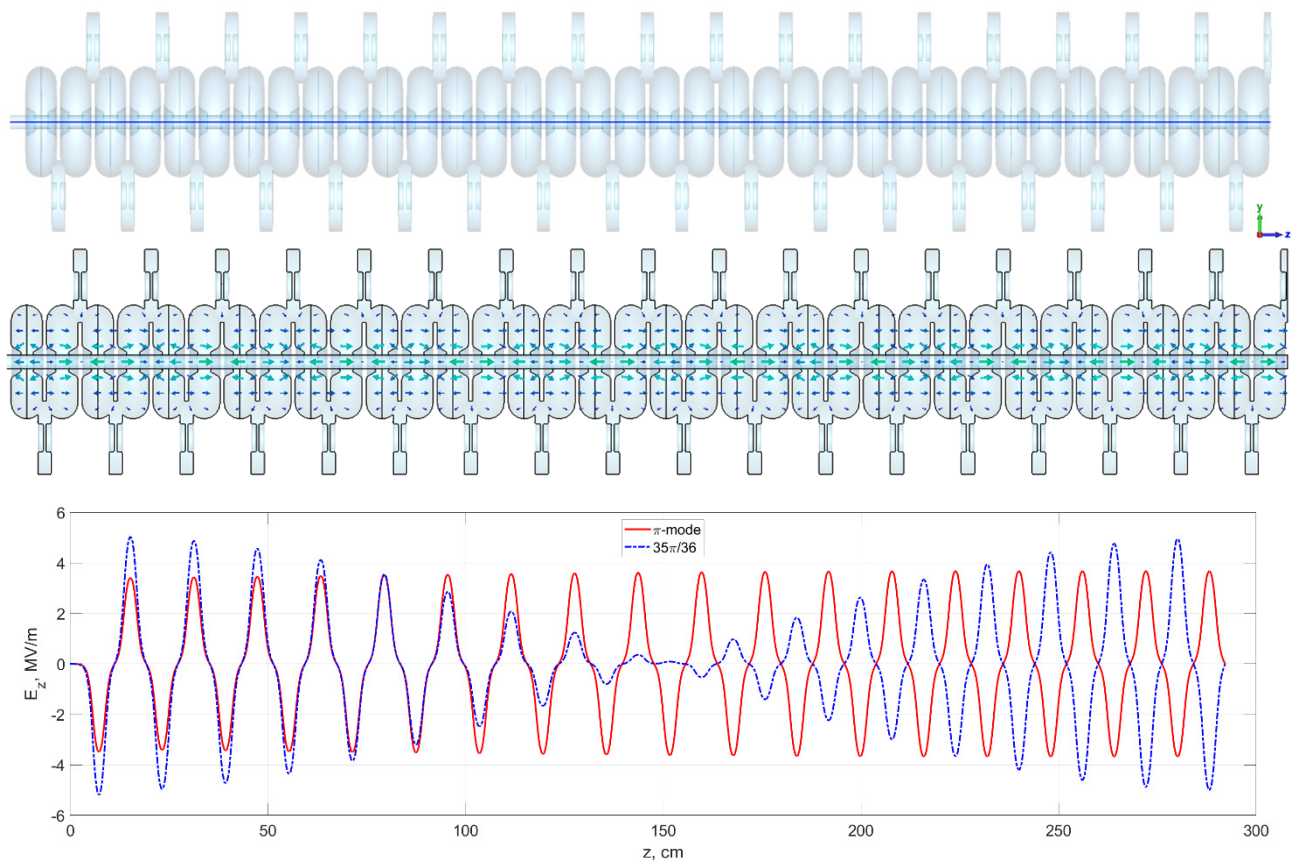


Figure 2: From top: side view of the vacuum volume of M5T1 (36 AC); electric field of the operating π -mode; on-axis longitudinal electric fields of the two lowest modes: π -mode (red) and mode $35/36 \pi$ per AC (blue dashed).

The end cell at the tank exit, on the right side of Fig. 2, is connected to the bridge coupler. To avoid simulating the coupler, we simplified the tank model by imposing magnetic boundary in the mid-plane of the last CC. This simplification allows us to close the model and calculate all the tank modes. Figure 2 (bottom) shows the on-axis fields of the two lowest modes. The second lowest mode has a field phase advance of $35/36 \pi$ per AC, so that its field acquires a phase shift of $-\pi$ by the tank end, compared to the π -mode. This mode frequency is 46 kHz above that of the π -mode, about twice the mode resonance half-width, 23 kHz.

Magnetic Quadrupole Doublet

The drift after each CCL tank contains an EM quadrupole doublet. Bridge couplers displaced from the beam axis electromagnetically couple CCL tanks over the drifts and feed RF power into tanks. Previously, we used hard-edge approximation of quad fields for modeling beam dynamics in CCL [1]. Now we calculate the quad magnetic fields with CST EM Studio using a simplified CAD model of the quad doublet 05QD02 in the drift after M5T1; it is shown in Fig. 3. The on-axis spacing between the quad centers is 20 cm, the beam pipe aperture radius is $a = 1.5875$ cm. The current coils (copper color in Fig. 3) are close to each other. Nevertheless, the calculated fields show a rather small overlap, except in the space between two quads.

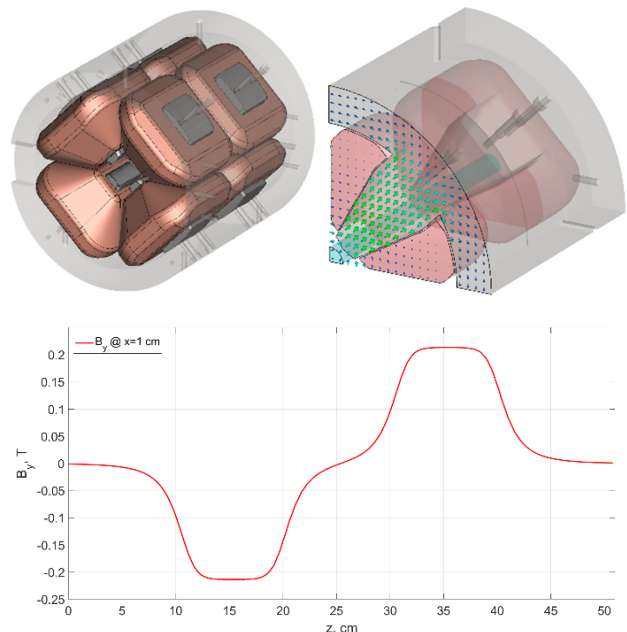


Figure 3: Top: CST model of quad doublet with yoke transparent (left); B-field arrows in the mid-pole cross section in one-quarter of the doublet (right). Bottom: By component on the line ($x = 1$ cm, $y = 0$).

We analyzed the harmonic content of the calculated quad field. The multipole coefficients a_n , b_n are defined as [5]

$$B(w) = B_y + iB_x = B_{ref} \sum_{n=1}^{\infty} (b_n + ia_n) (w/a)^{n-1}$$

in the complex w -plane, $w = x + iy$. Here $|B_{ref}| = 0.34$ T at the reference radius $a = 1.5875$ cm in the quad midplanes. The main calculated coefficients, normalized to the quadrupoles ($a_2 = 3.8 \cdot 10^{-4}$, $b_2 = 0.9959$), are listed in Table 2. The leading non-linear multipole – normal duodecapole term with coefficient b_6 – was included in Beampath runs.

Table 2: Multipole Coefficients of Quadrupole Doublet

Multipole n	a_n/a_2	b_n/b_2
1	0	$-1.39 \cdot 10^{-10}$
4	$5.39 \cdot 10^{-5}$	$-3.09 \cdot 10^{-4}$
6	$2.22 \cdot 10^{-2}$	$4.54 \cdot 10^{-3}$
8	$-1.03 \cdot 10^{-5}$	$-6.68 \cdot 10^{-5}$
10	$7.49 \cdot 10^{-4}$	$1.53 \cdot 10^{-4}$

PIC Modeling with CST Particle Studio

Using the calculated RF and quadrupole magnetic fields, we model beam dynamics in M5T1 with CST Particle Studio (PS) Particle-in-Cell (PIC) solver. The RF fields are extracted from eigensolver in the beam region, scaled to the T1 nominal gradient, and imported into PS. Details of PIC simulations and particle distributions used are described in [1]. Our main interest here was to study if the realistic quad fields give results different from the hard-edge approximations used previously [1]. For the considered well-matched beam distributions of 50K macro-particles, the results are practically the same. The input and output beam parameters are summarized in Table 3. It lists transverse normalized rms and longitudinal rms emittances, in π mm-mrad. The column “Out/In” lists ratios of final to initial parameters without misalignments; column “Out1/In” gives these ratios with misalignments included in PS simulations as described in [1].

Table 3: M5T1 Beam Parameters from PIC Simulations

Parameter	In	Out/In	Out1/In
Particles	50,000	1	1
Average energy, MeV	100	1.0342	1.0341
Tr. emittance ε_x , $\pi \mu\text{m}$	0.3687	1.0081	1.0098
Tr. emittance ε_y , $\pi \mu\text{m}$	0.3589	1.0093	1.0213
Longit. emitt. ε_z , $\pi \mu\text{m}$	1.7464	1.0033	1.0036
rms bunch length, deg	6.460	1.153	1.144
rms energy spread, MeV	0.2455	0.920	0.926

These results agree very well with those from Beampath simulations for this tank, M5T1, both without and with misalignments. This agreement gives us an additional confidence to trust Beampath for detailed simulations of the LANSCE CCL.

The initial and final particle distributions – at the CCL entrance, 100 MeV, and the exit, 800 MeV – generated by Beampath are used for developing robust physics-based surrogate models of the linac. HenonNet [6], a symplectic machine-learning (ML) surrogate model, was trained on the data for a few sets of linac parameters. It can reliably interpolate and predict results, so far in the longitudinal phase space, for different parameter values in a fraction of second, see in [6].

CONCLUSION

We developed simplified 3D CST models of CCL tanks of the LANSCE linac. The CST model for Tank 1 of Module 5 (M5T1), the first tank in the CCL linac, is studied. The 3D RF fields of tank modes are calculated with CST MicroWave Studio, quadrupole doublet magnetic fields – with EM Studio. Beam dynamics is modeled using the PIC solver in CST Particle Studio for bunch trains with a matched initial beam distribution. The PIC simulations use imported CST calculated RF and quadrupole magnetic fields. The beam emittance growth in M5T1 is rather small, which can be expected since the structure is relatively short, and the initial particle distribution was well matched. The measured misalignments, when added to the model, contribute to the emittance growth, cf. Table 3. CST modelling results for M5T1 are in good agreement with the results of Beampath simulations, both without and with misalignments. The beam dynamics results are used for developing robust physics-based surrogate models of the LANSCE coupled-cavity linac. We plan to extend beam dynamics simulations using more realistic beam particle distributions by modeling the transition region between the drift-tube linac and CCL.

Development of ML surrogate models for linac beam dynamics is supported by the LANL LDRD program.

REFERENCES

- [1] S. S. Kurennoy and Y. K. Batygin, “CST Modeling of the LANSCE Coupled-Cavity Linac”, in *Proc. 31st Int. Linear Accelerator Conf. (LINAC'22)*, Liverpool, UK, Aug.-Sep. 2022, pp. 191-193. doi:10.18429/JACoW-LINAC2022-MOPOGE17.
- [2] CST Studio, Dassault Systèmes: www.3ds.com/products-services/simulia/products/cst-studio-suite/
- [3] L. N. Engel, “Geometrical and Electromagnetic Parameters of the Accelerating and Coupling Cells of the 805 MHz Linac for LAMPF”, LANL, Los Alamos, NM, USA, Rep. MP-3-58, 1968.
- [4] Y. K. Batygin, “Particle-in-cell code BEAMPATH for beam dynamics simulations in linear accelerators and beamlines,” *Nucl. Instr. Meth. A*, vol. 539, pp. 455–489, 2005. doi:10.1016/j.nima.2004.10.029
- [5] Alexander Wu Chao, Karl Hubert Mess, Maury Tigner, Frank Zimmermann, *Handbook of Accelerator Physics and Engineering*, 2nd Ed., World Sci., May 2013, Sec. 6.17.1. doi:10.1142/8543
- [6] C. K. Huang *et al*, “Symplectic Neural Surrogate Models for Beam Dynamics,” presented at IPAC'23, Venice, Italy; paper WEP078; accepted *Jour. Phys.: Conf. Ser.*